ELSEVIER

P3HT/PCBM bulk heterojunction solar cells: Relation between morphology and electro-optical characteristics

P. Vanlaeke[a,b,*], A. Swinnen[b], I. Haeldermans[b], G. Vanhoyland[b], T. Aernouts[a], D. Cheyns[a], C. Deibel[a], J. D'Haen[a], P. Heremans[a], J. Poortmans[a], J.V. Manca[a,b]

[a]Imec vzw, Divisions MCP and IMOMEC, Kapeldreef 75, B-3001 Leuven, Belgium
[b]Universiteit Hasselt, Instituut voor Materiaalonderzoek, Wetenschapspark 1, B-3590 Diepenbeek, Belgium

Abstract

The performance of organic solar cells based on the blend of regioregular poly(3-hexylthiophene) (P3HT) and phenyl-C61-butyric acid methyl ester (PCBM) is strongly influenced by blend composition and thermal annealing conditions. X-ray diffraction (XRD) and Transmission Electron Microscopy (TEM) diffraction measurements show that in the considered blends, ordering of P3HT plays a key role in understanding the PV-performance. It is demonstrated that the natural tendency of regioregular P3HT to crystallize is disturbed by the addition of PCBM. Annealing however improves the crystallinity, explaining the observed spectral broadening and is also resulting in a higher mobility of the holes in P3HT.
© 2006 Elsevier B.V. All rights reserved.

*Corresponding author. Imec vzw, Divisions MCP and IMOMEC, Kapeldreef 75, B-3001 Leuven, Belgium. Tel.: +32 16 281590; fax: +32 16 281097.
E-mail address: vanlaeke@imec.be (P. Vanlaeke).

1. Introduction

Many different organic solar cell structures are currently being studied worldwide, but the donor/acceptor bulk heterojunction polymer solar cell is generally considered as the most promising approach. The advantages of this fully organic solar cell are that a good charge carrier collection is obtained by the interpenetrating network of donor and acceptor material and that the constituents are solution processible, which can make production potentially very inexpensive. In this type of structure the absorption of light results in excitons (bound electron hole pairs), which are split into free carriers at the interface between the donor and the acceptor material. The electron is transferred to the acceptor and the hole remains on the donor. After the exciton splitting, hole and electron transport occurs through respectively the donor and acceptor material towards the electrodes. The structure mostly is composed of a light absorbing donor polymer and a soluble C60 bucky ball derivative, typically phenyl-c61-butyric acid methyl ester (PCBM), acting as an acceptor. The main focus in the organic solar cell research lies on increasing the power conversion efficiency [1]. Since it has not yet been possible to replace the C60 derivatives with equally efficient electron acceptors, the preferred way to improve the solar cell efficiency is through the choice of the polymer [2,3]. Ideally the sun's maximum photon flux, lying around 650–700 nm, should be covered. Recently, semi crystalline regioregular poly(3-hexylthiophene) (P3HT) has attracted a lot of attention as a donor material, as it has an absorption edge around 650 nm, combined with a high hole mobility exceeding $0.1 \, cm^2/V \, s$ [4]. For these reasons the P3HT/PCBM system resulted in an improvement over the extensively studied poly(p-phenylene vinylene) (PPV) polymer/PCBM system [5,6].

Indeed, promising power conversion efficiencies, well over 3%, have been reported for P3HT based solar cells [7,8]. It also has been demonstrated that an annealing step is necessary to enhance the device performance. Much effort is put in understanding the device physics and optimising the efficiency of those cells [9–14].

A prerequisite for optimising the efficiency is understanding the relation between morphology and efficiency. This relationship has been studied experimentally in PPV based solar cells [15–18]. It was found that the interface between donor and acceptor should be as large as possible to have good charge carrier generation. Secondly, in the active layer blend networks of the donor and acceptor are required to have an efficient charge carrier extraction. Hereby, the blend ratio of the donor and acceptor material and the solvent used for production of the active layer are important parameters.

In this work, we present a combined morphological and electro-optical study of the P3HT based bulk heterojunction polymer solar cell. It will be shown further that in this material system, besides the points stated above, the crystallisation of the P3HT plays an important role in the device performance.

2. Results and discussion

From solar cells made in this study with different blend ratios of P3HT and PCBM spin coated from chlorobenzene solution it was concluded that the best power conversion efficiencies could be obtained from blends with 1:1 and 1:2 weight ratios. Post-production thermal annealing was applied to improve the efficiency as proposed by Padinger et al. [7]. The optimum annealing conditions for our samples were found to be 100 °C for 5 min.
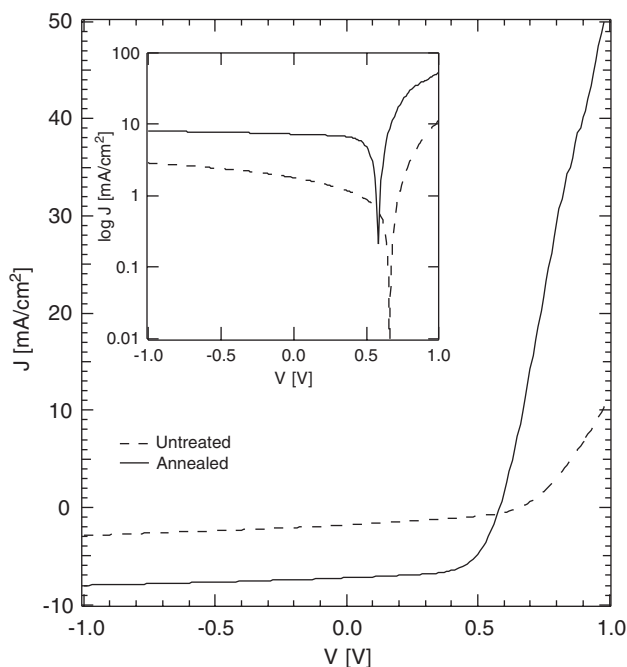
Fig. 1. I–V curve of a P3HT:PCBM 1:2 blend solar cell before and after annealing. The power conversion efficiency of the as-produced cell: 0.45% ($I_{sc} = 1.79$ mA/cm^2, $V_{oc} = 0.66$ V, fill factor = 38.4%); the power conversion efficiency of the annealed cell: 2.7% ($I_{sc} = 7.24$ mA/cm^2, $V_{oc} = 0.58$ V, fill factor = 64.0%).

Fig. 1 shows the effect of annealing on the current–voltage characteristics of a 1:2 blend based solar cell. The short circuit current and the fill factor are improved due to annealing, while the open-circuit voltage slightly decreases (contrary to the observations of Padinger et al. [7], who observed an increase in open-circuit voltage). Maximum efficiencies under 100 mW/cm^2 white light illumination were similar for 1:1 and 1:2 blend solar cells and found to be 2.7%. In experiments comparing 1:1 with 1:2 blend solar cells, the 1:1 blend shows a better efficiency on average.

A first clear visual observation is that upon annealing the active layer changes colour from orange/brown to purple/red. Quantitative information is given in Fig. 2 where the effect of different annealing temperatures, ranging from 70 °C to 100 °C, is shown on the UV–Vis absorption spectrum of a 1:2 blend film. In the spectra, absorption caused by P3HT is visible between 400 and 650 nm, below 400 nm the absorption of PCBM is dominant. Illustrative spectra of pristine regiorandom and regioregular P3HT films are also included in Fig. 2.

The spectra obtained from annealing below 70 °C—not shown for reasons of clarity—did not result in any changes compared to the as-produced film. With annealing temperatures above 70 °C one can observe a progressive broadening of the spectra towards longer wavelengths with increasing annealing temperature. The resulting broader absorption spectrum of the solar cell is beneficial for the short-circuit current especially since after annealing the cell absorbs more closely to the maximum photonflux in the solar spectrum, lying around 700 nm.
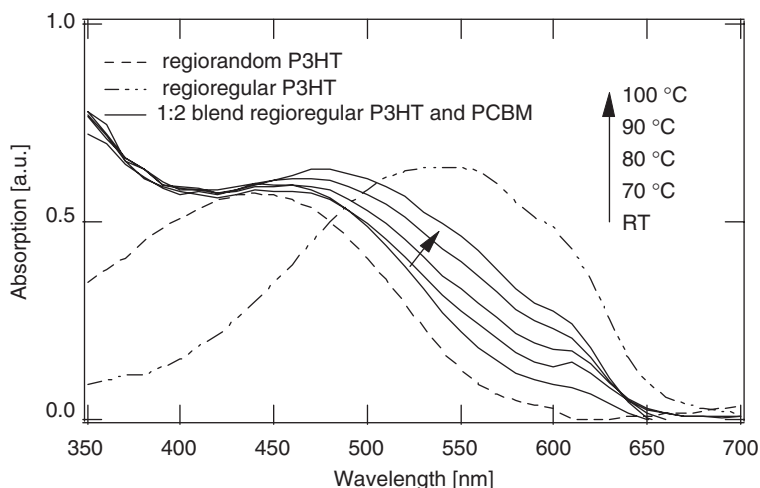
Fig. 2. UV–Vis spectra of the P3HT:PCBM 1:2 blend annealed at various temperatures. Illustrative spectra of pristine regiorandom and regioregular P3HT films are included.
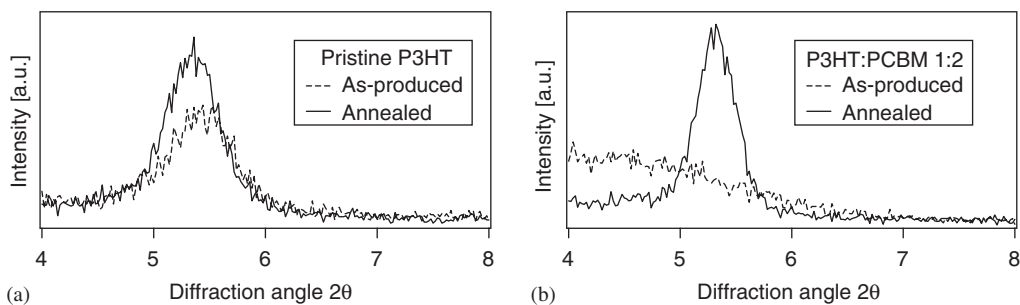

Fig. 3. XRD patterns of (a) pristine P3HT film and (b) P3HT:PCBM 1:2 blend film before and after annealing for 5 min at 100 °C.

Further, it was noticed that the absorption spectrum of as-produced blend films resembles more the absorption spectrum of amorphous regiorandom P3HT, whereas that of the annealed films resembles more closely the absorption spectrum of crystalline regioregular P3HT. These data are therefore a first indication that annealing improves the ordering of the P3HT phase.

Since organisation of the P3HT molecules in crystalline domains is expected from the UV–Vis data, diffraction spectra were recorded to get a more detailed picture.

X-ray diffraction spectra were taken from various as-produced and annealed blends. The results of the pristine P3HT film and the 1:2 blend film are presented in Fig. 3.

The spectrum for the as-produced pristine P3HT clearly shows the presence of a crystalline phase, which is further increased upon annealing. In the measurement range between 0° and 30° the signal of only one crystal plane was observed. An important result for the blended films is that the systematic addition of PCBM increasingly perturbs the formation of crystalline domains. The pristine P3HT and 1:1 blend show a crystalline peak around a 2θ value of 5.4°, representing an interplanar distance (d-spacing) of 1.61 nm. In

contrast, the P3HT in as-produced films with higher PCBM contents, such as 1:2 blends and 1:4 blends is in the amorphous phase. Interestingly, annealing could increase the crystallinity of all films. More specifically, for the amorphous as-deposited 1:2 blend and 1:4 blend crystallinity could be induced upon annealing.

Fig. 4 shows the TEM diffraction results for the 1:2 blend before and after annealing. Several broad peaks appear in Fig. 4, which correspond to diffraction rings, with average d-spacings at 0.46, 0.31 and 0.21 nm arising from nanocrystalline PCBM domains present in the blend [19]. After annealing a distinct peak is observable at 0.38 nm, which is attributed to crystalline P3HT [20].

With TEMdiffraction, the same trend was observed as with XRD: for blends with higher PCBM content the P3HT in the as-produced films is increasingly amorphous in nature and annealing can introduce or improve the crystallisation of P3HT. However, whereas XRD reveals only a d-spacing of 1.61 nm, TEM shows a spacing of 0.38 nm. This is not a contradiction but can be attributed to the preferential orientation of the P3HT molecules on the substrate [21]. Where XRD was measured in reflection and reveals d-spacings normal to the surface, TEM measures in transmission and gives d-spacings perpendicular to the surface. The d-spacing of 1.61 nm, as seen in XRD, can be attributed to twice the hexyl side chain length, representing the stacking of different P3HT molecules perpendicular to the substrate surface. The 0.38 nm spacing, measured with TEM, represents the π–π intramolecular stacking, parallel to the surface, of the thiophene into lamellae [22–24]. It was mentioned above that PCBM diffraction peaks were observed in the TEM diffraction spectra but not in the XRD spectra. The interpretation given for this observation is that the presumed preferred orientation of PCBM nanocrystals in the blended film could be induced by the observed preferred orientation of the surrounding P3HT. However, in order to come to definitive conclusions regarding this interpretation, this issue should be addressed with high energy synchroton radiation experiments.
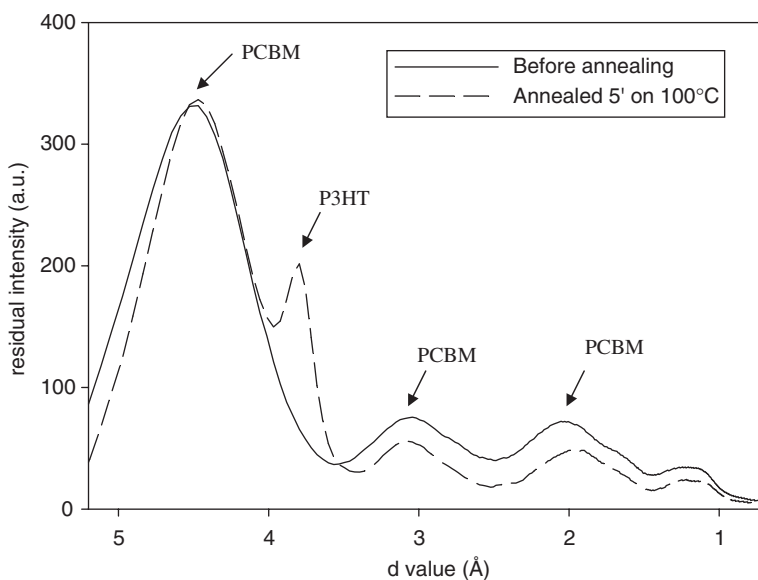

Fig. 4. TEM diffraction patterns of P3HT:PCBM 1:2 blend before and after annealing.

The TEM images presented in Fig. 5 were taken from a 1:1 blend film before and after annealing at $100\,^{\circ}C$ for 5 min. The as-produced film shows a smooth, homogeneous morphology, whereas the annealed film shows distinct rod-like P3HT crystals. The dimensions of the rods are around 10×30 nm. This corresponds to the results from the PPV based solar cell research where a phase separation of 30 nm or less was found to be optimal for exciton harvesting and charge carrier collection [16]. A PCBM phase above the detection limit of the microscope was not observed. However, PCBM nanocrystals must be present, since they were observed in the diffraction data.

At this point, after the presentation of the UV–Vis data and morphological results we can return to the discussion on the influence of annealing on the photovoltaic performance. There is no doubt that broadening of the absorption spectrum towards longer wavelengths due to crystallization of the P3HT has a positive impact on the short circuit current. The impact of the spectral broadening was estimated from spectral response measurements by Padinger et al. to be around 10%. The remaining part of the increase was attributed without proof to an increase in mobility [7]. We addressed this issue by extracting mobilities from field-effect transistor (FET) measurements based on 1:2 blend films annealed at different temperatures. Both hole and electron mobilities were determined. This was done to get an idea whether there is sufficient network formation including separate electron and hole channels with balanced carrier mobilities.

Fig. 6 shows the averaged results of hole mobilities determined from field-effect transistors operated in the saturation regime. Mobilities are plotted versus annealing temperatures. The annealing time was 5 min for every sample. It can be clearly seen that the hole mobility in P3HT:PCBM blends increases with increasing annealing temperatures, correlated with the increased crystallization of the P3HT. Moreover, the observed threshold temperature after which the effect of annealing becomes visible, agrees well with the threshold temperature observed in the UV–Vis spectroscopy measurements mentioned above. We observed that the effect of annealing is less pronounced on the measured electron mobility in the blend films. Electron mobilities in the order of $10^{-5}\,cm^2/V\,s$ have been obtained for the 1:2 blend. Hole and electron mobilities in a 1:2 blend film are fairly
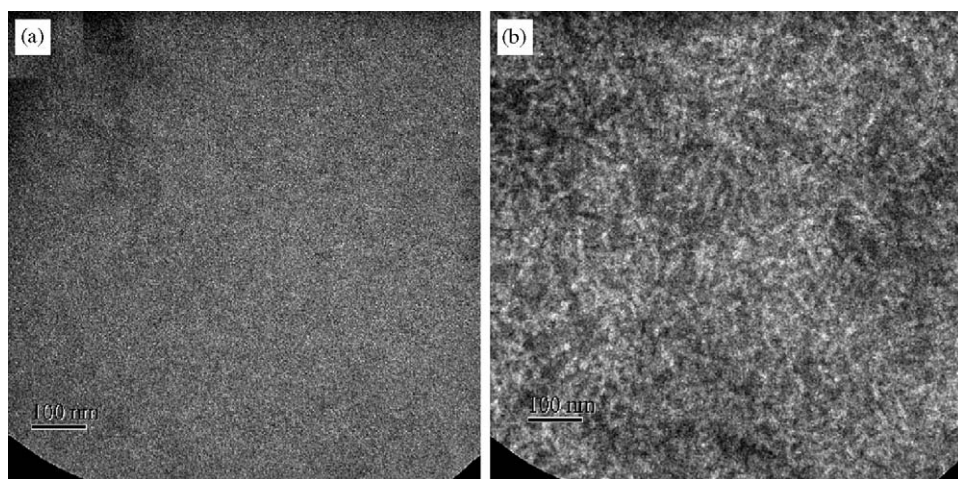

Fig. 5. TEM images of a P3HT:PCBM 1:1 blend (a) before and (b) after annealing at $100\,^{\circ}C$ for 5 min.
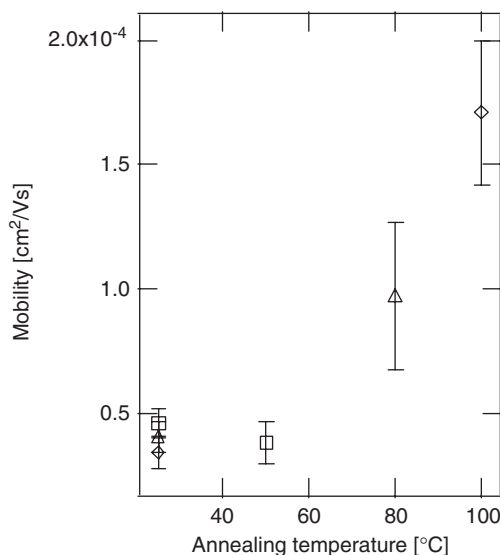
Fig. 6. FET hole mobilities in P3HT:PCBM 1:2 blends, as-produced and after annealing at various temperatures.

well balanced. This demonstrates the existence of a sufficient network of hole and electron channels.

3. Conclusions

It was shown that the beneficial effect of annealing on the solar cell performance is related with morphology changes and their implications. TEM and XRD results indicate that annealing induces an increased degree of crystallinity. The crystallinity of the as-produced films, however, depends on blend composition. Crystalline behaviour is observed in the as-produced films made from pristine P3HT and 1:1 blends. The as-produced blends containing more PCBM, appear to be amorphous. These results clarify the observed spectroscopic effect of broadening of the absorption spectrum after annealing. The broader absorption range is beneficial for the short circuit current in the solar cells. The d-spacings obtained with XRD and TEM indicate a preferred orientation of the P3HT on the sample surface. From field-effect transistor measurements it was shown that crystallisation of the P3HT not only has a beneficial spectroscopic effect, but also improves the hole mobility of blend films.

4. Experimental

The solar cell structures were prepared according to the following procedure. The ITO coated glass substrates, purchased from Merck Display Technologies with $\leqslant 20\,\Omega$/square, were first cleaned thoroughly with solvents and oxygen plasma treatment. By spin coating, the cleaned substrates were covered with a 30 nm thick layer of poly(3,4-ethylenediox-ythiophene):poly(styrenesulfonate) (PEDOT:PSS), purchased from HC Starck. The PEDOT layer was subsequently annealed in ambient at 120 °C for 10 min. The further

production and current/voltage characterization occurred in a nitrogen filled glove box system. The active layer containing a mixture of regioregular poly(3-hexylthiophene) (P3HT), purchased from Rieke Metals, and 1-(3-methoxycarbonyl)-propyl-1-phenyl-(6,6)C61 (PCBM), purchased from Nano-C Inc, was spin coated from chlorobenzene solution, which had been stirring on a hotplate at 50 °C. LiF (0.6 nm) and Al (100 nm) top electrodes were deposited by thermal evaporation in ultra high vacuum (10^{-6} Pa) through a shadow mask to define eight separate cells on one device. Solar cell active areas between 2.5 and 4 mm^2 were obtained and were exactly measured for each device using an optical microscope with measurement software. Thermal treatment was performed by putting the devices on a digitally controlled PMC 710 series Dataplate hotplate at 100 °C for 5 min.

The photovoltaic characteristics were measured with an Agilent 4156C parameter analyser under 100 mW/cm^2 white light illumination using a Fiber Lite PL-900 DC regulated illuminator with a 150 W halogen light source.

UV/Vis Transmission spectra were recorded using monochromated light from a Tungsten light source. Transmitted light was captured by an integrating sphere and detected by a combined Si and Ge detector.

X-ray diffraction (XRD) patterns were recorded using a Siemens D5000 diffractometer using Cu Kα1 (0.154056 nm) radiation.

For the TEM measurements thin freestanding films were prepared. TEM experiments were performed with a Philips CM12-STEM.

The field-effect transistor structures were made by spin coating the organic layer on n^{++} Si/Al substrates, used as gate, with 100 nm of thermally grown oxide as gate dielectric. LiF/Al source and drain electrodes were evaporated on top of the organic layer. The channel width was 2 mm, the channel lengths varied between 75 and 200 μm. Mobilities were extracted from the saturation regime.

Acknowledgements

References

[1] P. Peumans, A. Yakimov, S.R. Forrest, J. Appl. Phys. 93 (2003) 3693.
[2] C. Winder, N.S. Sariciftci, J. Mater. Chem. 14 (2004) 1077.
[3] J. Nelson, Current Opin. Solid State Mater. Sci. 6 (2002) 87.
[4] D.H. Kim, Y.D. Park, Y.S. Jang, H.C. Yang, Y.H. Kim, J.I. Han, D.G. Moon, S.J. Park, T.Y. Chang, C.W. Chang, M.K. Joo, C.Y. Ryu, K.W. Cho, Adv. Func. Mat. 15 (2005) 77.
[5] C.J. Brabec, N.S. Sariciftci, J.C. Hummelen, Adv. Func. Mat. 11 (2001) 15.
[6] H. Spanggaard, F.C. Krebs, Sol. Energy Mater. Sol. Cells 83 (2004) 125.
[7] F. Padinger, R.S. Rittberger, N.S. Sariciftci, Adv. Func. Mat. 13 (2003) 85.
[8] C.J. Brabec, Sol. Energy Mater. Sol. Cells 83 (2004) 273.
[9] D. Chirvase, Z. Chiguvare, M. Knipper, J. Parisi, V. Dyakonov, J.C. Hummelen, J. Appl. Phys. 93 (2003) 3376.
[10] I. Riedel, V. Dyakonov, Phys. Status Solidi A 201 (2004) 1332.
[11] P. Schilinsky, C. Waldauf, J. Hauch, C.J. Brabec, J. Appl. Phys. 95 (2004) 2816.
[12] K. Inoue, R. Ulbricht, P. Madakasira, W. Sampson, S. Lee, J. Gutierrez, J. Ferraris, A. Zakhidov, Proc. SPIE 5520 (2004) 256.

[13] Y. Kim, S.A. Choulis, J. Nelson, D.D.C. Bradley, S. Cook, J.R. Durrant, Appl. Phys. Lett. 86 (2005) Art. No. 063502.
[14] D. Chirvase, J. Parisi, J.C. Hummelen, V. Dyakonov, Nanotechnology 15 (2004) 1317.
[15] S.E. Shaheen, C.J. Brabec, N.S. Sariciftci, F. Padinger, T. Fromherz, J.C. Hummelen, Appl. Phys. Lett. 78 (2001) 841.
[16] T. Martens, J. D'Haen, T. Munters, Z. Beelen, L. Goris, J. Manca, M. D'Olieslaeger, D. Vanderzande, L. De Schepper, R. Andriessen, Synth. Met. 138 (2003) 243.
[17] J.K.J. van Duren, X.N. Yang, J. Loos, C.W.T. Bulle-Lieuwma, A.B. Sieval, J.C. Hummelen, R.A.J. Janssen, Adv. Func. Mat. 14 (2004) 425.
[18] H. Hoppe, M. Niggemann, C. Winder, J. Kraut, R. Hiesgen, A. Hinsch, D. Meissner, N.S. Sariciftci, Adv. Func. Mat. 14 (2004) 1005.
[19] M.T. Rispens, A. Meetsma, R. Rittberger, C.J. Brabec, N.S. Sariciftci, J.C. Hummelen, Chem. Commun. 17 (2003) 2116.
[20] S. Hugger, R. Thomann, T. Heinzel, T. Thurn-Albrecht, Colloid Polym. Sci. 282 (2004) 932.
[21] Z. Bao, A. Dodabalapur, A.J. Lovinger, Appl. Phys. Lett. 69 (1996) 4108.
[22] T.A. Chen, X. Wu, R.D. Rieke, J. Am. Chem. Soc. 117 (1995) 233.
[23] K.J. Ihn, J. Moulton, P. Smith, J. Polym. Sci. Polym. Phys. Ed. 31 (1993) 735.
[24] H. Sirringhaus, P.J. Brown, R.H. Friend, M.M. Nielsen, K. Bechgaard, B.M.W. Langeveld-Voss, A.J.H. Spiering, R.A.J. Janssen, E.W. Meijer, P. Herwig, D.M. de Leeuw, Nature 401 (1999) 685.